NACA RM E50F21

NACA

RESEARCH MEMORANDUM

PENETRATION OF LIQUID JETS INTO A HIGH-VELOCITY AIR STREAM

By Louis J. Chelko

Lewis Flight Propulsion Laboratory
Cleveland, Ohio

NATIONAL ADVISORY COMMITTEE
FOR AERONAUTICS

WASHINGTON
August 14, 1950

NACA RM E50F21

NATIONAL ADVISORY COMMITTEE FOR AERONAUTICS

RESEARCH MEMORANDUM

PENETRATION OF LIQUID JETS INTO A HIGH-VELOCITY AIR STREAM

By Louis J. Chelko

SUMMARY

An investigation of the penetration characteristics of liquid (water) jets directed approximately perpendicular to a high-velocity air stream was made and a correlation of the penetration length with the primary flow variables was obtained from an analysis of the data. The ranges of primary flow variables investigated included jet-nozzle orifice diameters from 0.0135 to 0.0625 inch, air-stream densities from 0.0805 to 0.1365 pound per cubic foot, and liquid-jet velocities from 168.1 to 229.0 feet per second. The air-stream velocity and liquid-jet density were approximately constant at 742 feet per second and 62 pounds per cubic foot, respectively, throughout the investigation.

The results of this analysis indicated that the correlation method was applicable to jet nozzles of the design investigated and permitted the prediction of the penetration length for any operating condition within the range of the investigation.

INTRODUCTION

Among the problems encountered during an investigation of thrust augmentation of turbojet engines at the NACA Lewis laboratory was the design of nozzles that would give known penetration when used for the injection of liquids into the various stages of an axial-flow compressor. Because information on the penetration characteristics of liquid jets was unavailable, a brief investigation was conducted in a small air-flow tunnel. The penetration characteristics of liquid (water) jets issuing from nozzles of various orifice diameters and with various liquid flows directed approximately perpendicular to a high-velocity air stream were investigated. This investigation was essentially a qualitative study of the relative penetration with different jet-nozzle sizes; penetration was determined primarily by visual observation. Although an extensive amount of data was not recorded and accuracy was not stressed, the data obtained from the

investigation are considered applicable to many other liquid-jet-penetration problems. Accordingly, the data were generalized by a method similar to that of reference 1 and are presented herein in a form suitable for convenient application.

This correlation permits the determination of the penetration length for jet nozzles covering a range of jet-nozzle orifice diameters, air-stream densities, liquid-jet velocities, and mixing distances.

SYMBOLS

The following symbols are used in this analysis:

a,b,c,d e,f,g	exponents
D_j	diameter of cylindrical orifice of jet nozzle, inches
h	depth of test section, inches
K	coefficient
l	length of jet penetration into air stream at distance s downstream of jet-nozzle center line, inches
s	mixing distance or distance downstream of jet-nozzle center line, inches
V_j	velocity of liquid jet, feet per second
V_0	velocity of air stream, feet per second
w	width of test section, inches
ρ_j	density of liquid jet, pounds per cubic foot
ρ_0	density of air stream, pounds per cubic foot
μ_j	viscosity of liquid jet, pounds per foot-second
μ_0	viscosity of air stream, pounds per foot-second

APPARATUS

The air tunnel, shown in figures 1 and 2, was designed to simulate approximately the air velocities and the flow-passage dimensions of a typical axial-flow turbojet-engine compressor. A two-dimensional bellmouthed nozzle having a 4-inch-square throat was installed at the test-section inlet. The test section was designed to permit investigations of the penetration lengths of liquid jets into air streams of various depths. The cross-sectional area at all stations along the test section was made constant in order to maintain constant air velocities through the bellmouthed nozzle throat and the test section; therefore, the width of the test section varied with its depth. Transparent lucite walls were installed on both sides of the air tunnel so that visual observation and photographic records of the liquid-jet penetration could be made. Jet nozzles were installed on the top of the test section at stations 1 and 2 (fig. 2); the corresponding test-section depths were 3.625 and 2.250 inches, respectively. Jet nozzles were mounted at station 1 either flush with the top of the test section (hereinafter called position 1a) or extended 2 inches into the air stream (hereinafter called position 1b). At station 2 the jet nozzles were installed flush with the top of the test section (position 2a).

Air was supplied by the laboratory services and was metered with an orifice installed in the supply duct. An auxiliary pump used in conjunction with an air-operated pressure regulator permitted control of the liquid flow and pressure to a supply header to which the jet nozzles were connected. Water was the only liquid used during this investigation.

Two types of jet nozzle of the same design except for the approach diameters were investigated. These two types of nozzle are designated type A and type B and are shown in figures 3(a) and 3(b), respectively. Both types of jet nozzle had 60° conical inlets followed by cylindrical orifices having length-to-diameter ratios of 0.50. This length-to-diameter ratio was found by preliminary experiments to give the best solid jet in still air for a large range of water flows. The cylindrical-orifice sizes, jet-nozzle diameters D_j, that were investigated for each type of nozzle are listed in figure 3.

The instrumentation, as shown in figure 2, consisted of a thermocouple pressure rake having two total-pressure tubes, a static-pressure tube, and two thermocouples installed at the

throat of the two-dimensional bellmouthed inlet nozzle and a thermocouple and a pressure tap installed in the water-supply header before the inlet to the jet nozzles.

PROCEDURE

The penetration lengths and the mixing distances of the liquid jets into the high-velocity air stream were determined from photographs taken through the transparent air-tunnel walls. The measurements were obtained with the aid of a scale that was installed in the same plane as the jet nozzle at the time the photographs were taken. For all the jet nozzles, the penetration length was arbitrarily chosen as the vertical distance from the outlet end of the jet nozzle to the outer visible boundary of the liquid jet at the corresponding mixing distance downstream of the jet-nozzle center line, as shown schematically in figure 4. Figures 5 and 6 are typical photographs showing the path of the liquid jets issuing from nozzles installed in positions 1a and 1b, respectively. Small distortions occurred in the photographs for different sets of data because the camera was not in the same position for all runs. These distortions, in addition to such effects as paper stretch and scale effect in the photographs, caused small inaccuracies in the penetration measurements.

The velocity and the density of the air stream (at temperatures of approximately 70° F) were constant throughout the length of the test section and were determined by using compressible-flow relations. The velocity of the liquid jet was determined by use of Bernoulli's theorem, assuming that the discharge coefficient was equal to 1.00. The effective differential pressure of the liquid across the jet nozzle was taken equal to the static pressure in the water-supply header minus the static pressure of the air in the test section. The density of the liquid jet was obtained by using the measured temperature of the liquid and the curves presented in reference 2. No provision was made for systematically varying the density of the water.

The investigation was conducted over the following range of conditions:

Jet-nozzle diameter D_j (in.)	Air-stream density ρ_0 (lb/cu ft)	Jet-nozzle type	Position
0.0625	0.081 - 0.132	A	1a
.0240 - .0625	.134	A	2a
.0135 - .0410	.081	B	1b

The liquid-jet velocity was varied over a range from approximately 168.1 to 229.0 feet per second for each set of conditions in the preceding table and the air-stream velocity and the liquid-jet density were approximately constant throughout the investigation at 742 feet per second and 62 pounds per cubic foot, respectively. These conditions are tabulated for each run in table I.

ANALYSIS

A simple dimensional analysis was made involving all the variables that may be expected to affect the penetration length l and the following expression was obtained:

$$\frac{l}{D_j} = K \left(\frac{\rho_j V_j D_j}{12\mu_j}\right)^a \left(\frac{V_j}{V_0}\right)^b \left(\frac{\rho_j}{\rho_0}\right)^c \left(\frac{\mu_j}{\mu_0}\right)^d \left(\frac{s}{D_j}\right)^e \left(\frac{w}{D_j}\right)^f \left(\frac{h}{D_j}\right)^g \qquad (1)$$

Equation (1) is similar to that presented in reference 1, where the penetration of air jets directed perpendicular to an air stream was investigated.

The effect of evaporation of the liquid was calculated for the various operating conditions investigated and was found to be of negligible magnitude and therefore was considered as not affecting the penetration length.

Although the limited scope of the present investigation was such that a separate study of each of the parameters in equation (1) was impossible, several of the parameters may be eliminated from consideration because they were either constant or were found to be of negligible magnitudes. Analysis of the data obtained at the two jet-nozzle positions indicated that the width and depth parameters w/D_j and h/D_j had no effect on the penetration length l within the range of the present data. Although the viscosity ratio μ_j/μ_0 varied because of variation in liquid-jet temperature (73° to 130° F),

no consistent effect of viscosity ratio on the penetration data could be observed; the effect of viscosity ratio therefore could not be evaluated from the present data. Also, for the range of jet Reynolds numbers $\rho_j V_j D_j / 12\mu_j$ investigated (10,000 to 150,000) no consistent trend in the penetration data with jet Reynolds number could be observed; therefore, it was considered that the jet Reynolds number effect must be small for the range of conditions covered and it was eliminated from the present analysis. Thus, all of the flow parameters except velocity ratio V_j/V_0, density ratio ρ_j/ρ_0, and mixing-distance jet-diameter ratio s/D_j were eliminated from equation (1) for the present analysis and the equation for the penetration parameter l/D_j reduces to

$$\frac{l}{D_j} = K\left(\frac{V_j}{V_0}\right)^b \left(\frac{\rho_j}{\rho_0}\right)^c \left(\frac{s}{D_j}\right)^e \tag{2}$$

When the coefficient K and the various exponents appearing in equation (2) are evaluated, an equation relating the penetration length l and the various operating conditions is obtained that serves to correlate the data and to permit the prediction of the penetration length for any velocity ratio, density ratio, and mixing-distance jet-diameter ratio for the range of conditions investigated.

EVALUATION OF EXPONENTS

Exponent b for velocity ratio V_j/V_0. - The variation of penetration parameter l/D_j with velocity ratio V_j/V_0 for three density ratios is presented in figure 7 for the type-A jet nozzle of 0.0625-inch diameter at a constant mixing-distance jet-diameter ratio s/D_j of 25.0 in position 1a. A straight line having a slope of 0.95 is drawn through the data for each of the density ratios. Although, for clarity of presentation, data are shown for only one jet-nozzle size, type, and position, data for all other sizes, types, and positions investigated also fell along straight lines with slopes of 0.95 for all density ratios. The logarithmic plot of figure 7 indicates that the exponent b for the velocity ratio is equal to 0.95 and equation (2) therefore becomes

$$\frac{l}{D_j} = K\left(\frac{V_j}{V_0}\right)^{0.95} \left(\frac{\rho_j}{\rho_0}\right)^c \left(\frac{s}{D_j}\right)^e \tag{3}$$

Exponent c for density ratio ρ_j/ρ_0. - A cross plot of figure 7 is shown in figure 8 in which the penetration parameter l/D_j is plotted as a function of density ratio ρ_j/ρ_0 for two velocity ratios. Straight lines with slopes of 0.74 are defined by this cross plot. Similar cross plots of the other jet-nozzle sizes, types, and positions gave the same result. This logarithmic cross plot therefore defines the exponent c for the density ratio as equal to 0.74 and equation (3) becomes

$$\frac{l}{D_j} = K\left(\frac{V_j}{V_0}\right)^{0.95}\left(\frac{\rho_j}{\rho_0}\right)^{0.74}\left(\frac{s}{D_j}\right)^{e} \tag{4}$$

Exponent e for mixing-distance jet-diameter ratio s/D_j. - In order to obtain the variation of the penetration parameter l/D_j with mixing-distance jet-diameter ratio s/D_j, a plot of l/D_j must be made for constant velocity ratio and density ratio. This plot was most conveniently obtained by a cross plot of figure 9, which presents the variation of the penetration parameter l/D_j with $\left(\frac{V_j}{V_0}\right)^{0.95}\left(\frac{\rho_j}{\rho_0}\right)^{0.74}$ for a range of constant mixing-distance jet-diameter ratios s/D_j from 8 to 74. Data for all the various jet-nozzle diameters for two jet-nozzle types, two positions, and two mixing distances are included in this figure to extend the range of the plot and to note their agreement at constant mixing-distance jet-diameter ratio s/D_j.

The logarithmic cross plot of figure 9 is presented in figure 10, which shows the variation of the penetration parameter l/D_j with mixing-distance jet-diameter ratio s/D_j for several values of $\left(\frac{V_j}{V_0}\right)^{0.95}\left(\frac{\rho_j}{\rho_0}\right)^{0.74}$. Straight lines with a common slope of 0.22 are defined from this cross plot and therefore the exponent e for the mixing-distance jet-diameter ratio is equal to 0.22 and equation (4) becomes

$$\frac{l}{D_j} = K\left(\frac{V_j}{V_0}\right)^{0.95}\left(\frac{\rho_j}{\rho_0}\right)^{0.74}\left(\frac{s}{D_j}\right)^{0.22} \tag{5}$$

FINAL CORRELATION

The final correlation, which is obtained by plotting the penetration parameter l/D_j against the factor $\left(\frac{V_j}{V_0}\right)^{0.95}\left(\frac{\rho_j}{\rho_0}\right)^{0.74}\left(\frac{s}{D_j}\right)^{0.22}$ on logarithmic coordinates, is presented in figure 11. The scatter of the data about the mean line is about ±7 percent, which is within the accuracy of the original photographic records.

The value of the coefficient K found by the substitution of the values of the coordinates of any point on the line in the correlation equation, is equal to 0.450. The final equation is accordingly written

$$\frac{l}{D_j} = 0.450\left(\frac{V_j}{V_0}\right)^{0.95}\left(\frac{\rho_j}{\rho_0}\right)^{0.74}\left(\frac{s}{D_j}\right)^{0.22} \qquad (6)$$

The data for type-A jet nozzle in position 1a are not included in figure 11 because they departed appreciably from the correlation of that figure. The correlation obtained with these data is illustrated in figure 12. These data are observed to correlate satisfactorily with the same exponents as the data of figure 11 but K is 19 percent higher (K = 0.535). The exact reason for this difference in the value of K is unknown but may be any one or a combination of the effects of differences in the air-stream boundary layers for different jet-nozzle immersions, velocity profiles, data inaccuracies, or photographic aberrations in the original records. Because the predominant amount of data falls on the curve of figure 11 and because these data were among the latest obtained and thus may have been subject to smaller errors due to experimental technique, the value of the coefficient K believed to be the most accurate and recommended for use is 0.450, as in equation (6).

SUMMARY OF RESULTS

From an analysis of data obtained on the penetration characteristics of liquid (water) jets directed approximately perpendicularly to a high-velocity air stream, a correlation method was obtained

that satisfactorily correlated the penetration data for jet nozzles of various throat diameters for a range of air-stream densities and liquid-jet velocities.

Lewis Flight Propulsion Laboratory,
National Advisory Committee for Aeronautics,
Cleveland, Ohio.

REFERENCES

1. Callaghan, Edmund E., and Ruggeri, Robert S.: Investigation of the Penetration of an Air Jet Directed Perpendicularly to an Air Stream. NACA TN 1615, 1948.

2. Anon.: Fluid Meters, Their Theory and Application. A.S.M.E. Res. Pub., Pub. by Am. Soc. Mech. Eng. (New York), 4th ed., 1937.

TABLE I - RANGES OF VARIABLES INVESTIGATED

Jet-nozzle diameter, D_j (in.)	Air-stream velocity, V_o (ft/sec)	Air-stream density, ρ_o (lb/cu ft)	Jet-nozzle type	Jet-nozzle position	Liquid jet velocity V_j (ft/sec)	Liquid jet density ρ_j (lb/cu ft)	Penetration length at s = 0.5 inch, l (in.)	Penetration length at s = 1.0 inch, l (in.)	Penetration length at s/D_j = 25.0, l (in.)
0.0625	753.7	0.1137	A	1a	169.9	62.16	1.30	1.60	1.70
.0625	752.7	.1137	A	1a	209.2	62.14	1.60	1.90	2.10
.0625	751.6	.1137	A	1a	224.6	62.15	1.65	2.00	2.20
.0625	749.0	.1153	A	1a	169.7	62.20	1.45	1.75	1.80
.0625	744.1	.1159	A	1a	209.0	62.16	1.70	2.05	2.20
.0625	740.2	.1162	A	1a	224.4	62.17	1.80	2.13	2.30
.0625	747.2	.1314	A	1a	168.4	62.15	1.20	1.44	1.58
.0625	737.7	.1321	A	1a	208.0	62.14	1.47	1.75	1.95
.0625	736.7	.1321	A	1a	223.4	62.14	1.55	1.90	2.06
.0625	735.9	.0815	A	1a	173.3	62.17	1.84	2.18	2.37
.0625	734.9	.0821	A	1a	226.6	62.11	2.37	2.77	2.98
.0625	735.5	.1359	A	2a	167.9	62.11	1.00	1.25	1.35
.0625	730.3	.1365	A	2a	223.0	62.11	1.34	1.62	1.75
.0469	751.3	.1330	A	2a	168.1	62.03	.80	.93	.98
.0469	746.3	.1343	A	2a	223.4	61.93	1.05	1.23	1.25
.0312	751.2	.1330	A	2a	169.6	61.90	.58	.68	.65
.0312	750.3	.1333	A	2a	225.6	61.74	.78	.90	.85
.0240	753.1	.1333	A	2a	169.6	61.69	.45	.54	.48
.0240	750.3	.1336	A	2a	225.4	61.61	.61	.72	.63
.0410	738.3	.0815	B	1b	172.8	61.86	1.10	1.28	1.30
.0410	740.3	.0811	B	1b	227.1	61.86	1.40	1.63	1.63
.0360	748.1	.0805	B	1b	172.1	62.09	1.00	1.15	1.13
.0360	742.2	.0808	B	1b	226.6	61.86	1.30	1.45	1.40
.0312	746.5	.0808	B	1b	171.2	62.28	.90	1.04	.98
.0312	742.6	.0811	B	1b	224.6	62.28	1.19	1.31	1.25
.0280	742.6	.0811	B	1b	171.2	62.28	.80	.93	.88
.0280	742.6	.0811	B	1b	224.9	62.28	1.08	1.22	1.15
.0250	744.5	.0811	B	1b	172.7	62.28	.75	.85	.78
.0250	742.6	.0811	B	1b	226.5	62.28	1.00	1.12	1.05
.0200	742.6	.0811	B	1b	174.5	62.28	.60	.70	.60
.0200	742.6	.0811	B	1b	229.0	62.28	.80	.90	.80
.0135	742.6	.0811	B	1b	173.0	62.28	.44	.50	.40
.0135	742.6	.0811	B	1b	226.4	62.28	.60	.67	.55

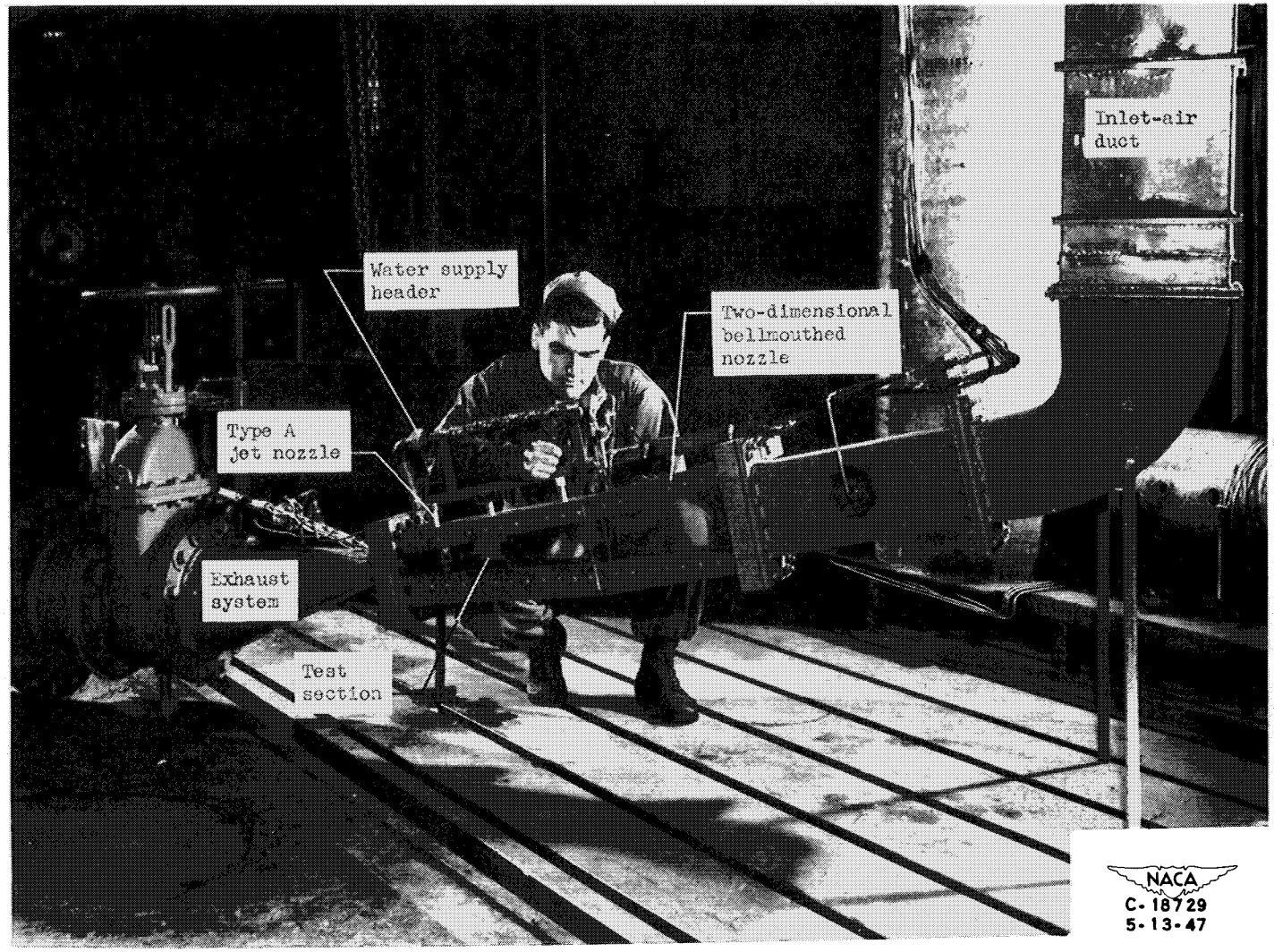

Figure 1. - Air-tunnel installation.

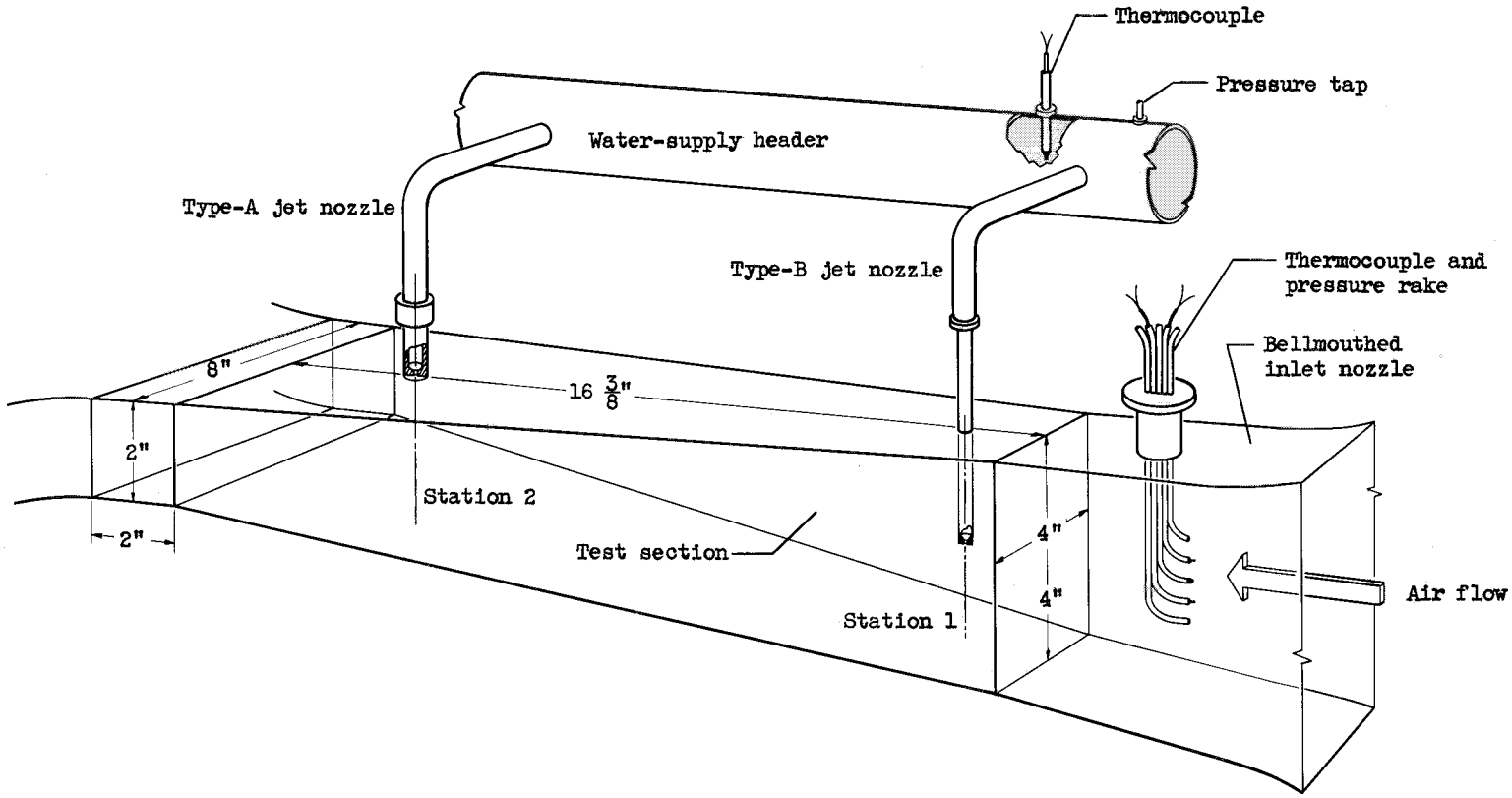

Figure 2. - Schematic diagram of air tunnel.

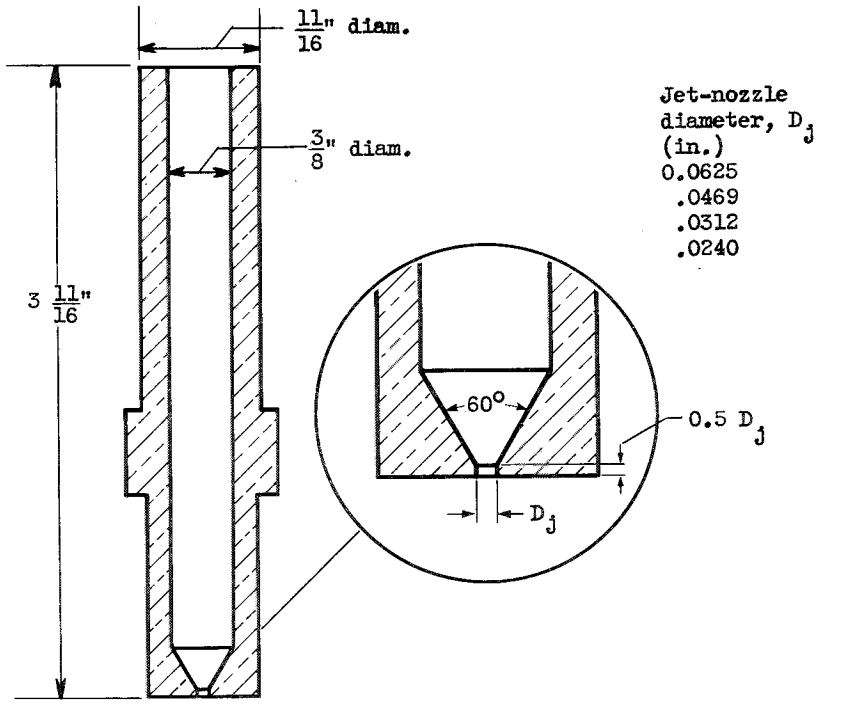

(a) Type A

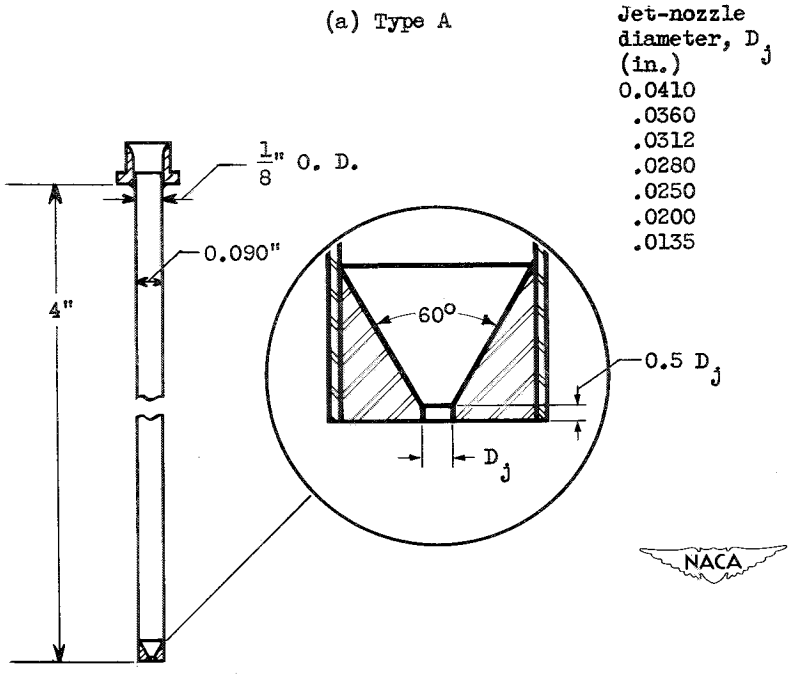

(b) Type B.

Figure 3. - Schematic diagram of jet nozzle.

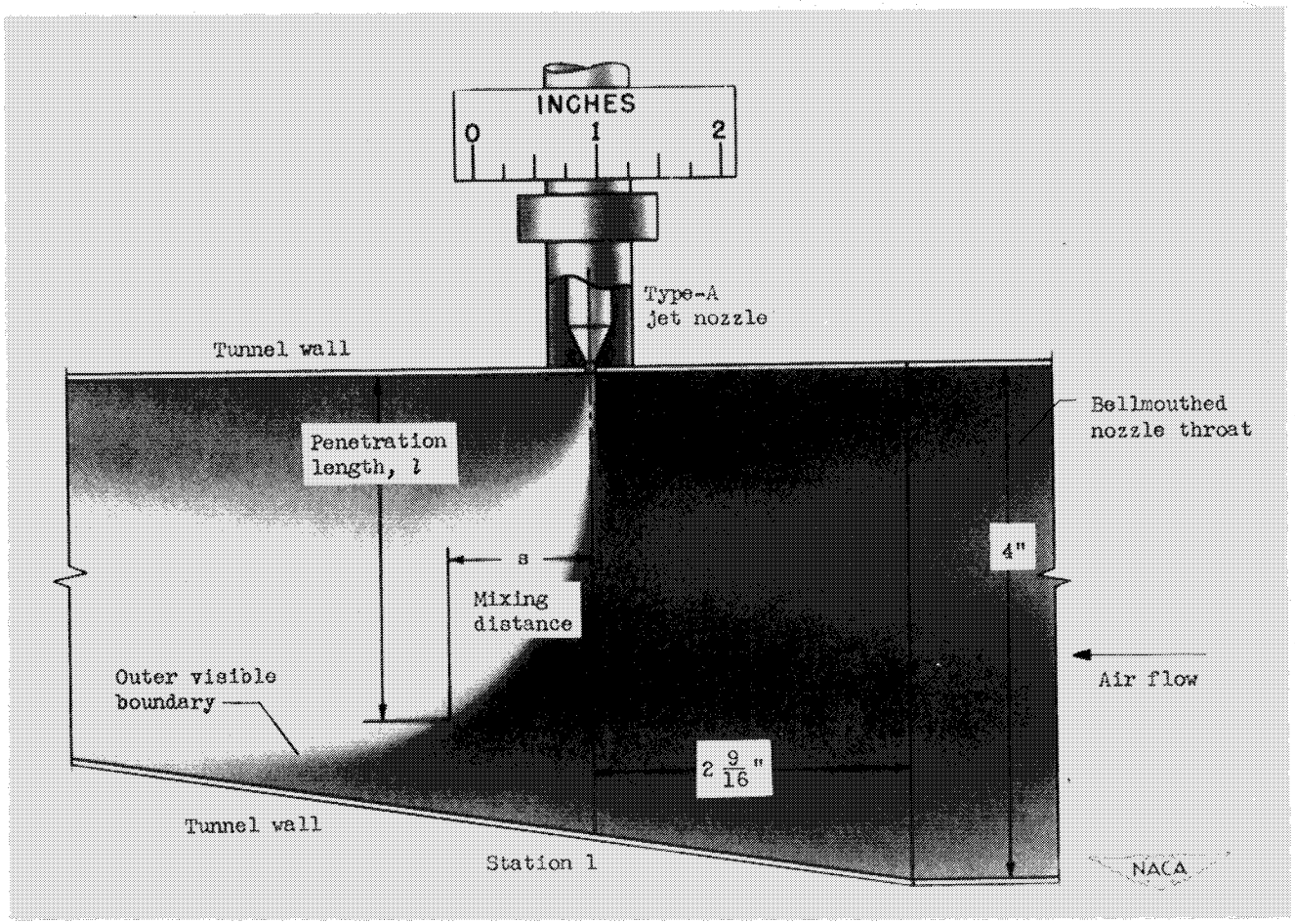

Figure 4. - Schematic diagram indicating method of measuring penetration length and mixing distance.

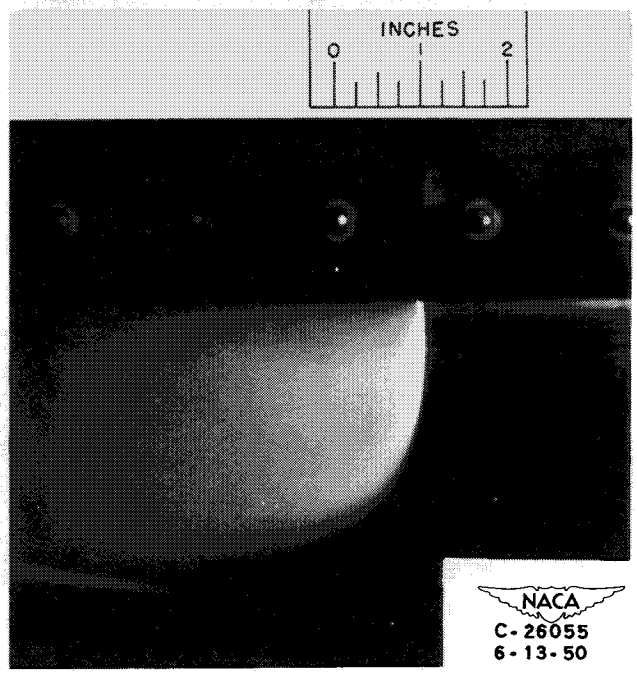

Figure 5. - Typical type A jet nozzle in position 1a. Jet-nozzle diameter, 0.0625 inch; air-stream velocity, 734.9 feet per second, air-stream density, 0.0821 pound per cubic foot; liquid-jet velocity, 226.6 feet per second; liquid-jet density, 62.11 pounds per cubic foot.

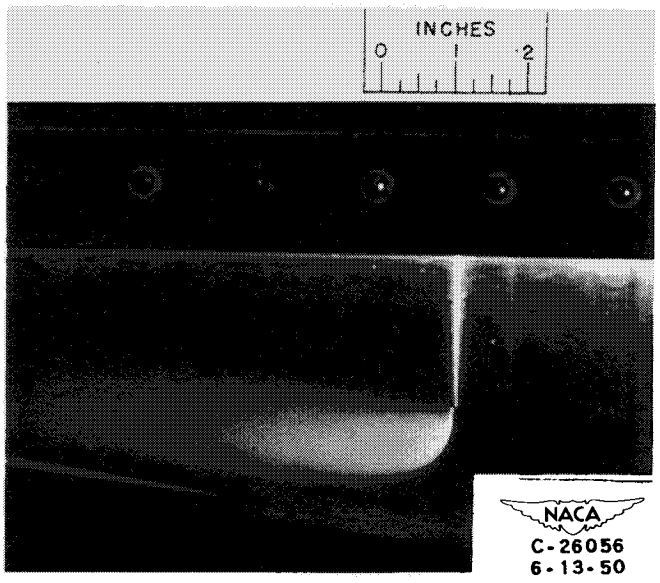

Figure 6. - Typical type B jet nozzle in position 1b. Jet-nozzle diameter, 0.0360 inch; air-stream velocity, 748.1 feet per second; air-stream density, 0.0805 pound per cubic foot; liquid-jet velocity, 172.1 feet per second; liquid-jet density, 62.09 62.09 pounds per cubic foot.

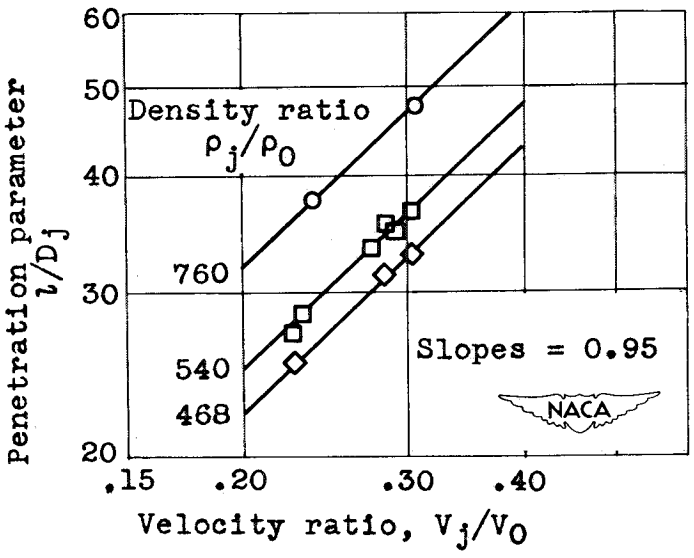

Figure 7. - Variation of penetration parameter with velocity ratio. Jet-nozzle type, A; jet-nozzle diameter, 0.0625 inch; mixing-distance jet-diameter ratio, 25.0; position, 1a.

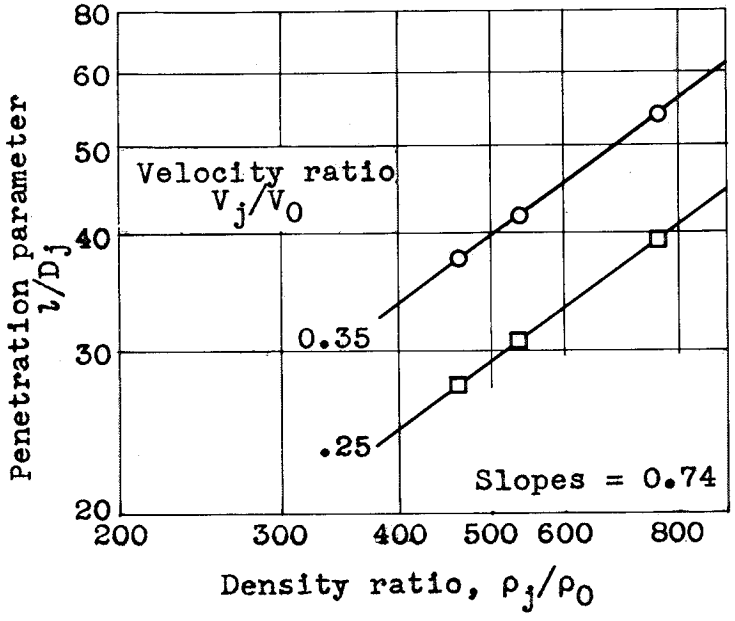

Figure 8. - Variation of penetration parameter with density ratio as obtained from cross plot of figure 7. Jet-nozzle type, A; jet-nozzle diameter, 0.0625 inch; mixing-distance jet-diameter ratio, 25.0; position, 1a.

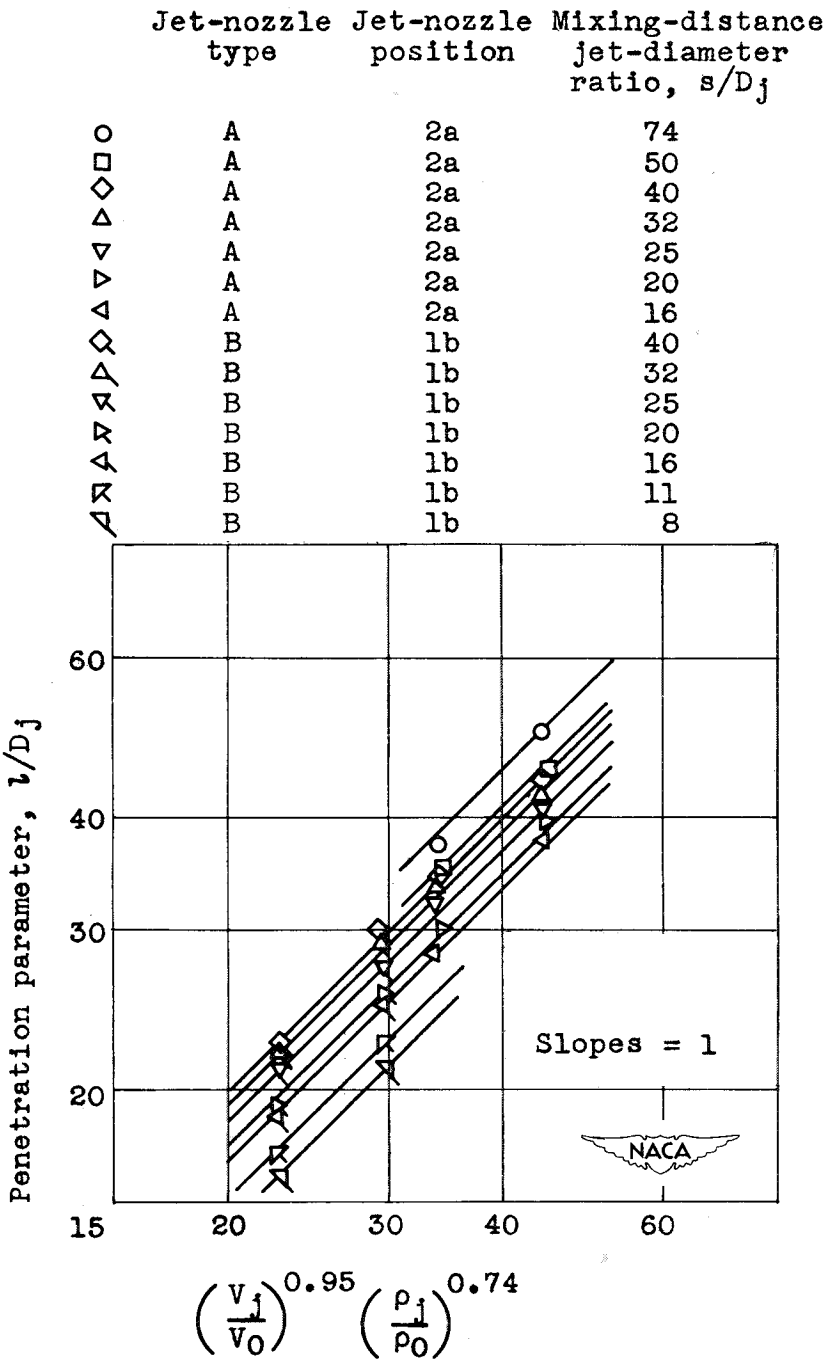

Figure 9. - Variation of penetration parameter with $(V_j/V_0)^{0.95}$ $(\rho_j/\rho_0)^{0.74}$ for various jet-nozzle diameters, type and position for range of mixing-distance jet-diameter ratios. Jet-nozzle diameters, 0.0135 to 0.0625 inch; mixing distances, 0.50 and 1.00 inch.

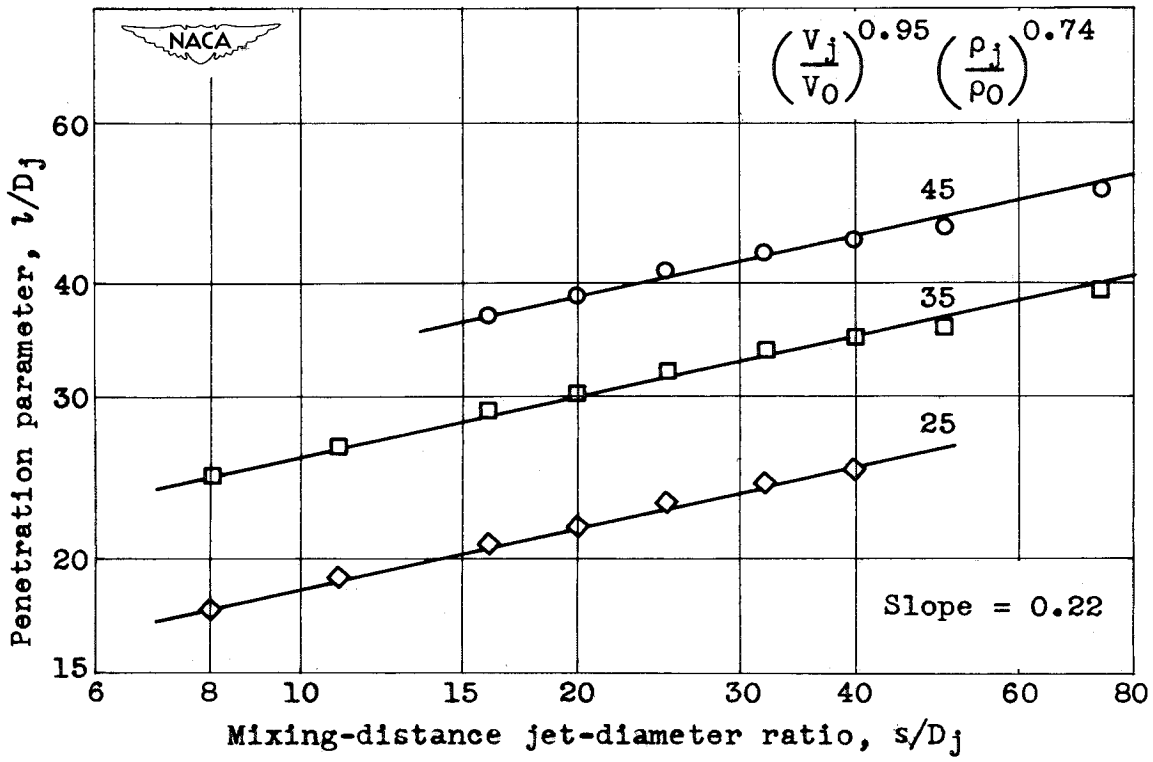

Figure 10. - Variation of penetration parameter with mixing-distance jet-diameter ratio as obtained from cross plot of figure 9. Jet-nozzle diameters, from 0.0135 to 0.0625 inch; mixing distances, 0.50 and 1.00 inch.

Jet-nozzle type B Position 1b			Jet-nozzle type A Position 2a		
	Jet diameter D_j	Mixing distance, s		Jet diameter D_j	Mixing distance, s
○	0.0410	1.00	□	0.0625	1.00
○	.0410	.50	□	.0625	.50
○	.0410	1.02	□	.0625	1.56
□	.0360	1.00	◇	.0469	1.00
□	.0360	.50	◇	.0469	.50
□	.0360	.90	◇	.0469	1.12
◇	.0312	1.00	◇	.0312	1.00
◇	.0312	.50	◇	.0312	.50
◇	.0312	.78	◇	.0312	.78
△	.0280	1.00	△	.0240	1.00
△	.0280	.60	△	.0240	.50
△	.0280	.70	△	.0240	.60
▽	.0250	1.00			
▽	.0250	.50			
▽	.0250	.63			
▽	.0200	1.00			
▽	.0200	.50			
△	.0135	1.00			
△	.0135	.50			
△	.0135	.34			

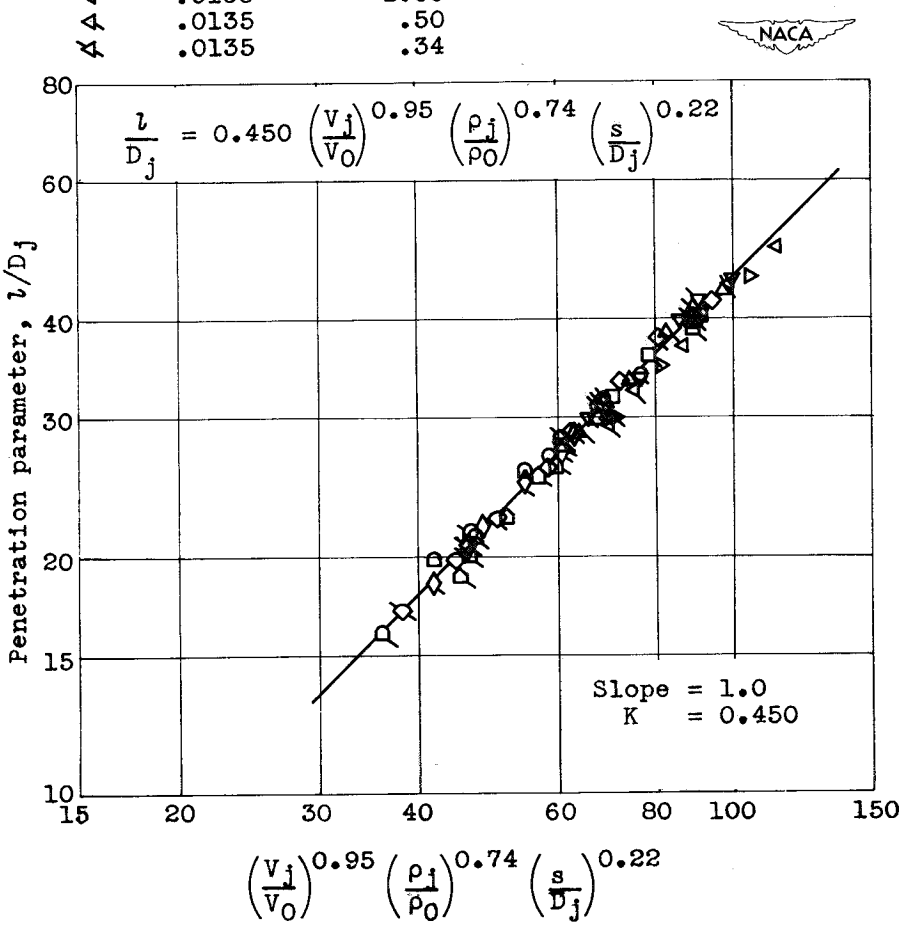

Figure 11. - Final correlation of penetration parameter.

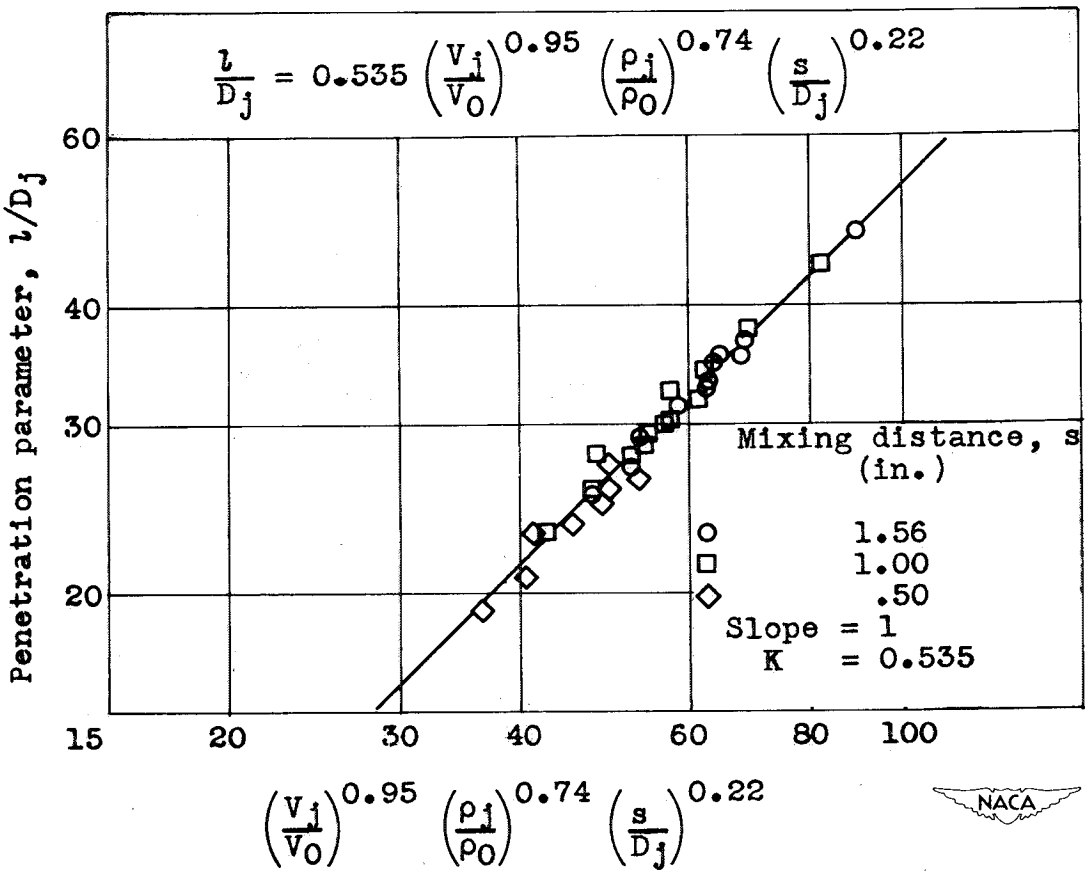

Figure 12. - Correlation of penetration parameter for jet-nozzle type A. Jet-nozzle diameter, 0.0625 inch; position, 1a.